



HAL
open science

Stimulated Emission up to 2.75 μm from HgCdTe/CdHgTe QW Structure at Room Temperature

Vladimir Utochkin, Konstantin Kudryavtsev, Alexander Dubinov, Mikhail Fadeev, Vladimir Rumyantsev, Anna Razova, Egor Andronov, Vladimir Ya. Aleshkin, Vladimir Gavrilenko, Nikolay Mikhailov, et al.

► **To cite this version:**

Vladimir Utochkin, Konstantin Kudryavtsev, Alexander Dubinov, Mikhail Fadeev, Vladimir Rumyantsev, et al.. Stimulated Emission up to 2.75 μm from HgCdTe/CdHgTe QW Structure at Room Temperature. *Nanomaterials*, 2022, 12 (15), pp.2599. 10.3390/nano12152599 . hal-03824966

HAL Id: hal-03824966

<https://hal.science/hal-03824966>

Submitted on 24 Oct 2022

HAL is a multi-disciplinary open access archive for the deposit and dissemination of scientific research documents, whether they are published or not. The documents may come from teaching and research institutions in France or abroad, or from public or private research centers.

L'archive ouverte pluridisciplinaire **HAL**, est destinée au dépôt et à la diffusion de documents scientifiques de niveau recherche, publiés ou non, émanant des établissements d'enseignement et de recherche français ou étrangers, des laboratoires publics ou privés.



Distributed under a Creative Commons Attribution 4.0 International License



Article

Stimulated Emission up to 2.75 μm from HgCdTe/CdHgTe QW Structure at Room Temperature

Vladimir V. Utochkin ^{1,*}, Konstantin E. Kudryavtsev ^{1,2}, Alexander A. Dubinov ^{1,2} , Mikhail A. Fadeev ¹ , Vladimir V. Rumyantsev ^{1,2} , Anna A. Razova ^{1,2}, Egor V. Andronov ^{1,3}, Vladimir Ya. Aleshkin ^{1,4}, Vladimir I. Gavrilenko ^{1,4}, Nikolay N. Mikhailov ⁵, Sergey A. Dvoretzky ⁵ , Frederic Teppe ⁶ and Sergey V. Morozov ^{1,2}

- ¹ Institute for Physics of Microstructures of RAS, 603950 Nizhny Novgorod, Russia; konstantin@ipmras.ru (K.E.K.); sanya@ipmras.ru (A.A.D.); fadeev@ipmras.ru (M.A.F.); rumyantsev@ipmras.ru (V.V.R.); annara@ipmras.ru (A.A.R.); andronov@ipmras.ru (E.V.A.); aleshkin@ipmras.ru (V.Y.A.); gavr@ipmras.ru (V.I.G.); more@ipmras.ru (S.V.M.)
- ² Faculty of Radiophysics, Lobachevsky State University, 603950 Nizhny Novgorod, Russia
- ³ Institute of Radio Electronics and Information Technologies, Nizhny Novgorod State Technical University n.a. R.E. Alekseev, 603950 Nizhny Novgorod, Russia
- ⁴ Advanced School of General and Applied Physics, Lobachevsky State University, 603950 Nizhny Novgorod, Russia
- ⁵ Institute of Semiconductor Physics, Siberian Branch of RAS, 630090 Novosibirsk, Russia; mikhailov@isp.nsc.ru (N.N.M.); dvor@isp.nsc.ru (S.A.D.)
- ⁶ Laboratoire Charles Coulomb, UMR 5221, CNRS-University of Montpellier, 34095 Montpellier, France; frederic.teppe@umontpellier.fr
- * Correspondence: utvlvas@ipmras.ru



Citation: Utochkin, V.V.; Kudryavtsev, K.E.; Dubinov, A.A.; Fadeev, M.A.; Rumyantsev, V.V.; Razova, A.A.; Andronov, E.V.; Aleshkin, V.Y.; Gavrilenko, V.I.; Mikhailov, N.N.; et al. Stimulated Emission up to 2.75 μm from HgCdTe/CdHgTe QW Structure at Room Temperature. *Nanomaterials* **2022**, *12*, 2599. <https://doi.org/10.3390/nano12152599>

Academic Editors: Huanjun Chen and Efrat Lifshitz

Received: 10 June 2022

Accepted: 26 July 2022

Published: 28 July 2022

Publisher's Note: MDPI stays neutral with regard to jurisdictional claims in published maps and institutional affiliations.



Copyright: © 2022 by the authors. Licensee MDPI, Basel, Switzerland. This article is an open access article distributed under the terms and conditions of the Creative Commons Attribution (CC BY) license (<https://creativecommons.org/licenses/by/4.0/>).

Abstract: Heterostructures with thin Hg(Cd)Te/CdHgTe quantum wells (QWs) are attractive for the development of mid-infrared interband lasers. Of particular interest are room-temperature operating emitters for the short-wavelength infrared range (SWIR, typically defined as 1.7–3 μm). In this work, we report on the observation of stimulated emission (SE) in the 2.65–2.75 μm wavelength range at room temperature in an optically pumped HgCdTe QW laser heterostructure. We study a series of three samples with lengths ranging from 2.5 to 7 mm and discuss the effects related to the non-uniformity of the excitation beam profile. SE threshold intensity and the magnitude of pump-induced carrier heating are found to be effectively dependent on the chip size, which should be accounted for in possible designs of HgCdTe-based optical converters. We also pay attention to the problem of active medium engineering in order to push the SE wavelength towards the 3–5 μm atmospheric window and to lower the SE threshold.

Keywords: HgCdTe; MCT; quantum well; stimulated emission; room temperature; mid-IR; carrier heating

1. Introduction

Developing compact, low-cost mid-infrared (mid-IR) lasers is crucial for many applications such as environmental monitoring, detection of carbohydrate derivatives, and medicine. The short-wavelength part of the IR range contains many absorption lines of gaseous pollutants and industrial and greenhouse gases, such as CO, CO₂, CH₄, nitrogen oxides, H₂S, H₂O, SO₂, and many others. Compact and efficient selective sensors for one or several substances can be realized by a combination of a tunable narrowband emitter and a nonselective detector, the technique known in literature as tunable laser absorption spectroscopy (TLAS). While the technology of mid-IR detectors is well developed, and there are many commercially available InGaAs-, InAs-, and HgCdTe-based detectors, the technology of low-cost tunable narrowband emitters is underdeveloped. Though there are many spectroscopic lines of various substances in the whole mid-IR range, researchers

focus on spectral ranges where atmospheric absorption is minimal, so-called atmospheric windows (0.8–2.5, 3–5, and 8–14 μm), because these ranges allow more accurate measurements by scanning larger volumes of air. Atmospheric absorption in the 2.5–3 μm range is determined predominantly by H_2O , CO , and CO_2 , so emitters in this range can be used for the sensing of the aforementioned gases [1–3]. As for water, biological tissues usually contain large amounts of it, and its strong absorption near 3 μm leads to a very low penetration depth in tissues, which finds applications in skin treatment, laser surgery, dentistry, and other medicine. Therefore, it is important to develop tunable semiconductor lasers that work at room temperature in the short-wavelength, mid-IR range from 2.5 to 5 μm .

Currently, experimentally demonstrated TLAS systems use interband cascade lasers based on III–V materials [4]. Interband cascade lasers provide continuous-wave emission at room temperature with up to 250 mW of output power [5]. At the same time, mass-production of cascade devices is still challenging due to complicated designs and high manufacturing costs. Contrary to this, type-I QW diode sources are easier to manufacture, and lasing with wavelengths above 2.5 μm was realized in semiconductor systems based on III–V (GaSb, InAs), IV–VI (PbS, PbSe), and II–VI ternary/quaternary alloys [6]. Currently, the longest wavelength of room-temperature emission achieved in III–V type-I QW diodes is equal to 3.5 μm [7]. Still, most of these material systems suffer from poor growth technology, which affects the durability and reproducibility of the sources.

In this regard, the sources based on mercury cadmium telluride (MCT, HgCdTe) are very compelling. HgCdTe technology is well developed and is used for the fabrication of IR detectors [8]; it is also considered a promising material for fabrication of mid-IR sources. Interband recombination and lasing in HgCdTe have been investigated since the mid-1960s [9]. However, room-temperature lasing was only achieved in the short-wavelength part of the mid-IR range (2.2 μm wavelength [10]), and, at longer wavelengths, the critical temperature T_{max} at which stimulated emission (SE) can be observed decreases rapidly; T_{max} was ~ 190 K for 2.6 μm lasing [11], while a 5.3 μm laser operated at temperature was as low as 45 K [12]. It is well established that the observed strong thermal quenching of interband lasing from narrow gap materials is related to the activation of non-radiative AR processes [12–14]. The AR rate increases with temperature and emission wavelength, which prevents room-temperature operation of the interband sources above a certain wavelength.

AR is a three-particle process in which an electron–hole pair recombines and transfers energy to the third carrier [15]; threshold “bulk-like” eeh AR involves two electrons from the lowest conductive subband and a hole from the highest valence subband without transitions to higher subbands. During the “bulk-like” Auger process, the total kinetic energy of the initial system has to exceed a certain threshold value to comply with energy and momentum conservation principles [16] (p. 191). It was demonstrated that implementation of thin Hg(Cd)Te/CdHgTe QWs with residual Cd in the QW material kept as low as possible within growth technique limitations could greatly suppress “bulk-like” AR [17]. Having implemented such thin QWs, we observed 3.8 μm SE at 240 K [18], 2.8 μm SE at 256 K [19], and 2.45 μm SE at room temperature [20] in “as-grown” planar structures, while the sample with fabricated microdisk resonators provided 4.1 μm SE at 260 K [21].

In this work, we modified the sample design from [20] by realizing slightly lower Cd content in the QWs and barrier layers in order to push the room-temperature SE wavelength further into the infrared, towards the 3–5 μm atmospheric window.

2. Materials and Methods

The structure studied was MBE grown on semi-insulating GaAs (013) substrate with ZnTe (50 nm thick) and CdTe (10 μm thick) buffers with in situ ellipsometric control of layer thickness and Cd content (see Figure 1). Typical growth parameters and the discussion of MBE process for growth of multiple HgCdTe QWs can be found in [22]. The structure contained 10 Hg_{0.82}Cd_{0.18}Te/Cd_{0.68}Hg_{0.32}Te QWs, each 2.7 nm thick in its active area, and was designed to effectively confine guided mode near the QW array, for which the QWs

were incorporated into a 800 nm $\text{Cd}_{0.68}\text{Hg}_{0.32}\text{Te}$ waveguide layer with approximately 900 meV bandgap.

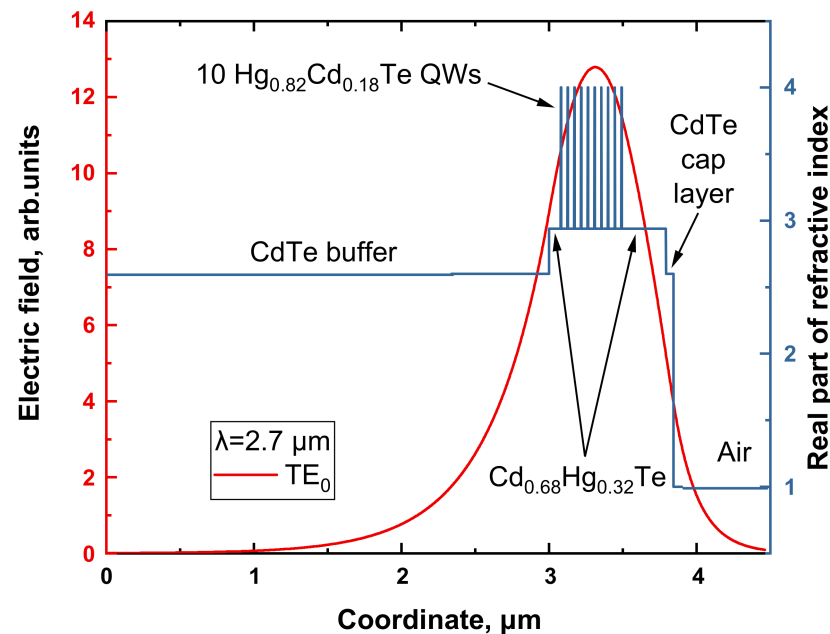


Figure 1. Distribution of real part of refractive index and TE₀ mode localization for the structure under study at the wavelength $\lambda = 2.7 \mu\text{m}$.

For PL and SE measurements, we chipped a series of three samples with lengths ranging from 2.5 mm to 7 mm (hereafter “2.5 mm”, “4 mm”, and “7 mm”) from the grown structure. For the initial sample characterization via spontaneous PL studies, a continuous-wave (CW) diode laser operating at 808 nm was used as an excitation source; pump density was about $10 \text{ W}/\text{cm}^2$. For SE spectra measurements, a near-IR optical parametric oscillator (OPO) was used, emitting an approximately $2 \mu\text{m}$ wavelength with an output energy of $\sim 10 \text{ mJ}$ in a 10 ns pulse and a repetition rate of 10 Hz. Pump intensity was attenuated using a set of neutral-density filters. Emitted light was collected from either the surface (for spontaneous PL) or from the cleaved facet (for SE) of the sample and analyzed by a Bruker Vertex 80v Fourier-transform spectrometer equipped with an MCT photodetector ($16 \mu\text{m}$ cut-off wavelength) and operating in the step-scan mode. During SE studies, the excitation spot completely covered the entire sample, and each sample was placed in the center of the laser spot. Note that due to a specific growth direction (013), naturally cleaved facets did not form a Fabry–Perot resonator, so we predominantly studied single-pass SE. Additional SE experiments were conducted with another excitation source, an OPO emitting at $1.6 \mu\text{m}$ (also 10 ns pulse and a repetition rate of 10 Hz), to allow direct comparison with results from [20]. However, in this case only the “2.5 mm” sample could be effectively excited due to much lower pulse energy ($\sim 1 \text{ mJ}$). All experiments were conducted at room temperature with the samples mounted on a bulk aluminum heatsink.

The scattered $1.6 \mu\text{m}$ OPO (i) excitation and 808 nm diode excitation were completely cut off by a Ge filter limiting the spectrometer range to $550\text{--}5600 \text{ cm}^{-1}$. However, we were unable to completely filter $2 \mu\text{m}$ OPO (ii) excitation from $2.7 \mu\text{m}$ SE, which greatly complicated spontaneous emission studies under pulsed excitation.

3. Results and Discussion

In Figure 2, we show a steady-state PL spectrum of the 2.5 mm sample under weak CW excitation alongside the emission spectra measured under pulsed $1.6 \mu\text{m}$ excitation (also used in our preceding work [20]). From the spontaneous PL, the band gap energy was estimated at $E_g \sim 450 \text{ meV}$, which corresponds to $\sim 18\%$ Cd content in the QWs—close to the value retrieved from in situ sample characterization. Under pulsed excitation, a weak,

broad, spontaneous emission spectrum could be observed at the lowest photon flux of $2 \times 10^{24} \text{ s}^{-1} \text{ cm}^{-2}$ with only a slight feature resembling the SE line, while, at higher pump densities, we observed rapid signal growth and spectrum narrowing down to $\sim 60 \text{ cm}^{-1}$ (for spontaneous PL, the full width at half maximum, FWHM, of the emission spectrum is $\sim 500 \text{ cm}^{-1}$), which marks the onset of stimulated emission. Note, again, that the excitation beam was focused into a $\sim 3 \text{ mm}$ spot to achieve sufficient pump intensity ($\geq 200 \text{ kW/cm}^2$) for SE generation, so we could only observe SE in the shortest 2.5 mm sample. The estimated SE threshold was about two times higher than the shorter-wavelength sample from [20], predominantly due to narrower E_g and, correspondingly, the lower Auger threshold energy E_{th} (~ 71 vs. $\sim 65 \text{ meV}$).

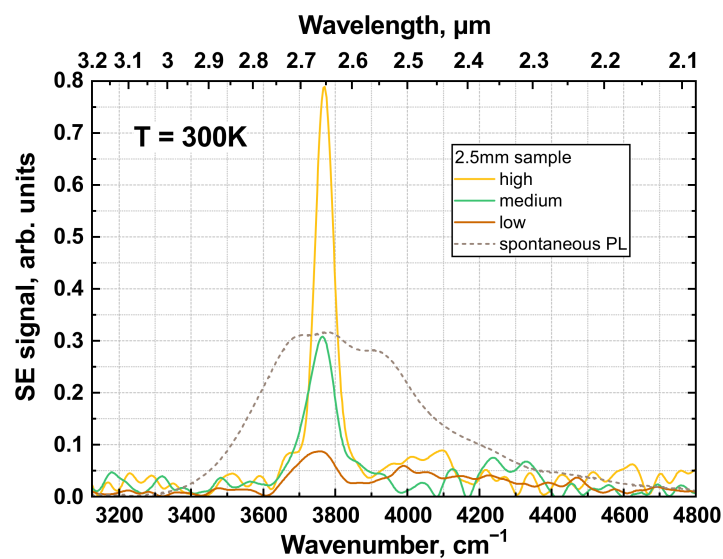


Figure 2. Stimulated emission (SE) spectra (solid lines) at $2.65 \mu\text{m}$ under various excitation intensities of $1.6 \mu\text{m}$ pulsed excitation (source (i)) and spontaneous emission spectrum under 808 nm continuous-wave diode excitation in the 2.5 mm sample. The low excitation intensity corresponded to less than $2 \times 10^{24} \text{ s}^{-1} \text{ cm}^{-2}$ photon flux, the medium one corresponded to $\sim (3 \div 3.5) \times 10^{24} \text{ s}^{-1} \text{ cm}^{-2}$ photon flux, and the high one to at least $4.5 \times 10^{24} \text{ s}^{-1} \text{ cm}^{-2}$ photon flux.

For more detailed studies, we switched to $2 \mu\text{m}$ OPO for the excitation of SE. With much higher pulse energy, it provided a photon flux high enough for SE generation in all samples and allowed accurate measurement of SE threshold intensities (see Figure 3). Note that, for the 2.5 mm sample, rather close SE thresholds were observed under $1.6 \mu\text{m}$ and $2 \mu\text{m}$ excitation at $\sim (2 \div 3) \times 10^{24} \text{ s}^{-1} \text{ cm}^{-2}$. While it was demonstrated in [20] that implementation of longer-wavelength excitation might lower the SE threshold, here, we did not see any pronounced effect. This can be explained given that the excitation wavelengths were both close to the SE wavelength ($2.7 \mu\text{m}$) and so the effects related to “hot-hole generation” (holes above the AR threshold, the concept proposed in [20]) and the strong heating of excess carriers at extreme pump levels (recently evaluated in [23]) were expected to be of minor importance. It should also be noted that both the $1.6 \mu\text{m}$ and $2 \mu\text{m}$ wavelengths corresponded to below-barrier excitation; based on measured transmittance spectra, we estimated direct absorption of the pump light in the QW array at some 8–10% at these wavelengths.

For each sample in the series, we measured SE spectra at several different excitation intensities determined by the set of optical filters. Experimental results are summarized in Figure 3. In panel (a), we show the integrated emission intensity depending on the excitation density; here, excitation photon fluxes for each sample were calculated, taking into account a Gaussian intensity profile of the pump laser beam ($\sim 6 \text{ mm}$ FWHM) and the exact position of the sample relative to the excitation spot (shorter samples at the center of the laser spot effectively had higher photon flux than longer samples under the same average excitation power).

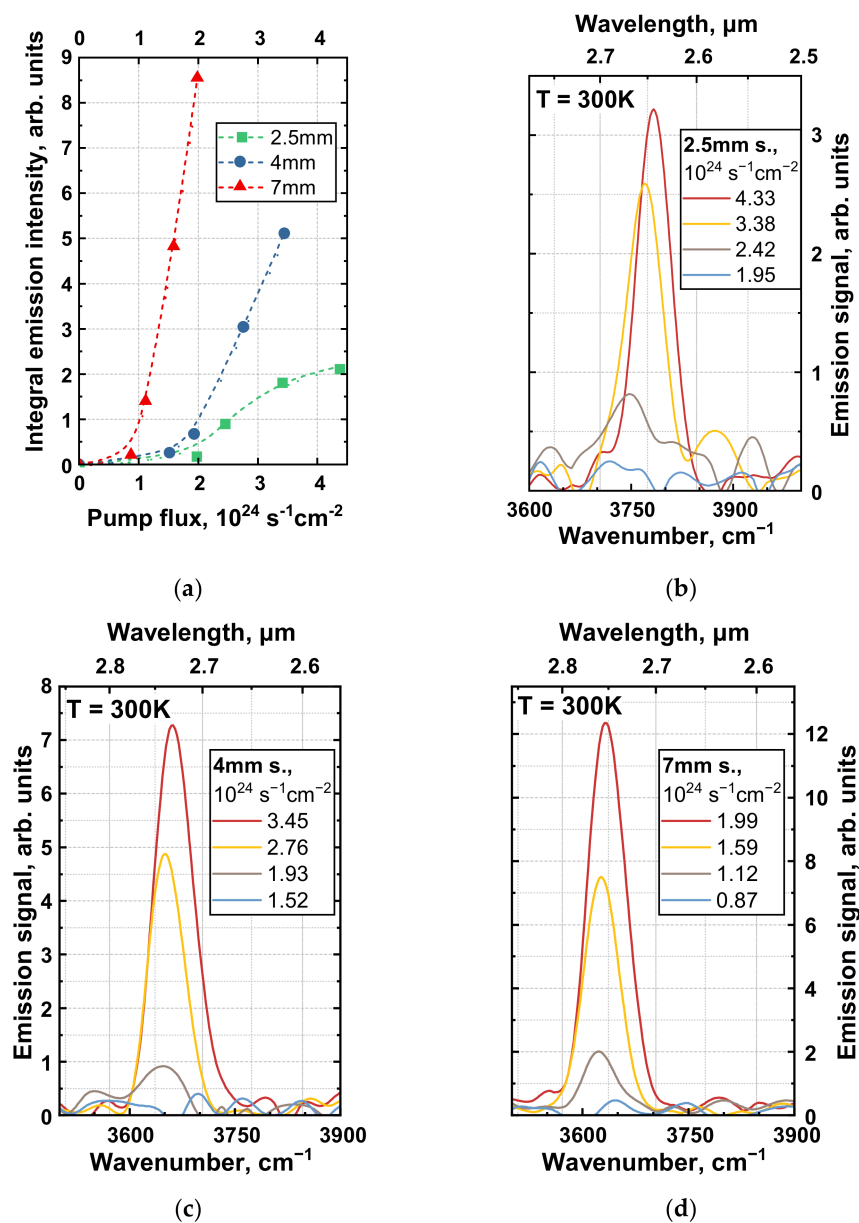


Figure 3. (a) Room-temperature light-in versus light-out (L–L curves) characteristics for each sample. Emission spectra of the (b) 2.5 mm sample, (c) 4 mm sample, (d) 7 mm sample under various excitation photon fluxes of the 2 μm pulsed excitation (source (ii)). Arbitrary units in (b–d) are the same for all three samples.

Clearly, luminescence had threshold dependence on the pump power, and samples of varying lengths exhibited different SE thresholds. Though there were minor variations in the band gap energies of the samples under study (see corresponding SE spectra in Figure 3b–d), it is not likely that interband recombination mechanisms and lasing thresholds were affected by this factor. Instead, we suggest that the observed differences in threshold intensities were directly related to the single-pass amplification regime, with longer samples allowing for a well-developed SE line at lower gain values. To provide rough estimates of material gain, we considered a one-dimensional amplifier model [24] and, based on the SE spectra given in Figure 3c,d, deduced gain values of $\sim 60 \text{ cm}^{-1}$ for the 7 mm sample at $1.6 \times 10^{24} \text{ s}^{-1} \text{ cm}^{-2}$ and $\sim 110 \text{ cm}^{-1}$ for the 4 mm sample at $2.75 \times 10^{24} \text{ s}^{-1} \text{ cm}^{-2}$ at the maximum of the SE line. Here, we accounted for an optical confinement factor of $\Gamma \sim 0.0355$, identical for all samples.

Obviously, the 2.5 mm sample required even higher optical gain (and, hence, excitation intensity) to achieve distinct SE, and it was difficult to give any reliable estimates for this sample. The first problem here was the rather poor signal-to-noise ratio. Second, more importantly, we observed saturation of the emission intensity and blueshift of the SE line in Figure 3a,b above $3 \times 10^{24} \text{ s}^{-1} \text{ cm}^{-2}$, indicating carrier overheating at given pump densities. For the 2.5 mm sample, Figure 3a looked like the left part of a “bell-shaped” L–L curve, which we often observed in mid-IR HgCdTe QW heterostructures at high excitation intensity and at temperatures close to the critical temperature of SE generation [23,25]. This result was in a good agreement with positions of the SE peaks (and correspondingly the maxima in the gain spectra were defined by the effective carrier temperature). Our previous experimental studies showed effective carrier temperature to be up to several times higher than the lattice temperature under the same 2 μm pumping as the excitation intensity increased beyond a certain value [23]. As the carrier temperature rises, the broadening of the gain spectrum triggers blueshift of the SE peak. The effect can hardly be avoided; however, its contribution can be minimized once dedicated photonic structures (e.g., Fabry–Perot cavities based on ridge waveguides) are fabricated. In this case, progressing from single-pass amplified spontaneous emission towards proper (multi-pass) lasing was expected to provide compact designs with a threshold intensity of less than $10^{24} \text{ s}^{-1} \text{ cm}^{-2}$, corresponding to less than 1.5 kA/cm² per QW under electrical pumping.

The given estimates for the threshold current of mid-IR HgCdTe lasers under consideration were definitely higher than those reported for III–V based lasers emitting at the same wavelength [26]. Still, HgCdTe may have certain possibilities for improvement. With a threshold flux at $10^{24} \text{ ph}/(\text{cm}^2 \text{ s})$ and a calculated QW transparency concentration of 10^{12} cm^{-2} , we followed [23] to evaluate the effective (2D) Auger coefficient at $10^{-14} \text{ cm}^4/\text{s}$, more than an order of magnitude higher than typically reported for III–V type-I QWs [26] and closely resembling “bulk” values. At the same time, QW-induced suppression of the Auger recombination at somewhat longer wavelengths was demonstrated in [18]. We suggest that the stronger AR in relatively wide gap samples studied in the current work might be related to the QW-specific processes with the excitation resulting in hot electrons in the continuum states above the barrier level (and it is exactly the process believed to be a limiting factor for high-temperature SE in [18]). While the energy threshold for conventional *eeh* AR (involving fundamental QW subbands) amounted to approximately 65 meV, we obtained about twice the lower value for barrier-assisted AR. Thus, tuning the latter process off-resonance by alternating barrier composition (and so the band offsets in the QW) may be helpful to mitigate related AR and reduce the lasing threshold to more practical levels.

4. Conclusions

We obtained stimulated emission at room temperature in the 2.65–2.75 μm range from a planar $\text{Hg}_{0.82}\text{Cd}_{0.18}\text{Te}/\text{Cd}_{0.6}\text{Hg}_{0.4}\text{Te}$ QW structure under pulsed optical excitation. While this region is not very convenient for spectroscopy of gases in the atmosphere due to fundamental absorption lines of water and CO_2 , there are some potential applications for the sensing of these gases in the range discussed and in medicine. In comparison with previous structure design [20], the emission wavelength was 0.3 μm longer, while the threshold intensity for SE generation was several times higher under both 1.6 μm and 2 μm excitation. This required new structure designs for propagating the SE wavelength of room-temperature HgCdTe optical converters towards the 3–5 μm atmospheric window, in particular, active medium engineering for lowering the SE threshold intensity. Having studied a series of three samples with varying lengths, we observed pump-induced carrier heating while measuring signal vs. pump curves, and the effect was clearly pronounced in the shortest sample. We attribute this effect to the non-uniformity of the excitation beam profile and considered cavity processing to mitigate it.

Author Contributions: Conceptualization, V.V.U., M.A.F. and S.V.M.; methodology, V.V.U. and M.A.F.; software, A.A.D. and V.Y.A.; validation, K.E.K. and F.T.; formal analysis, V.V.U., V.V.R. and A.A.D.; investigation, V.V.U., M.A.F., A.A.R. and E.V.A.; resources, N.N.M. and S.A.D.; data curation, A.A.R. and E.V.A.; writing—original draft preparation, V.V.U.; writing—review and editing, K.E.K. and F.T.; visualization, V.V.U. and V.V.R.; supervision, S.V.M.; project administration, S.V.M. and V.I.G.; funding acquisition, S.V.M. and V.I.G. All authors have read and agreed to the published version of the manuscript.

Funding: The work was supported by the Ministry of Science and Higher Education of the Russian Federation (grant #075-15-2020-797, agreement 13.1902.21.0024). This work was also supported by CNRS through IRP “TeraMIR” and by the French Agence Nationale pour la Recherche (Colector ANR-19-CE30-0032).

Institutional Review Board Statement: Not applicable.

Informed Consent Statement: Not applicable.

Data Availability Statement: The data presented in this study are available on request from the corresponding author.

Conflicts of Interest: The authors declare no conflict of interest. The funders had no role in the design of the study; in the collection, analyses, or interpretation of data; or in the writing of the manuscript or in the decision to publish the results.

References

1. Farooq, A.; Jeffries, J.B.; Hanson, R.K. CO₂ concentration and temperature sensor for combustion gases using diode-laser absorption near 2.7 μm. *Appl. Phys. B* **2008**, *90*, 619–628. [[CrossRef](#)]
2. Briggs, R.M.; Frez, C.; Bagheri, M.; Borgentun, C.E.; Gupta, J.A.; Witinski, M.F.; Anderson, J.G.; Forouhar, S. Single-mode 2.65 μm InGaAsSb/AlInGaAsSb laterally coupled distributed-feedback diode lasers for atmospheric gas detection. *Opt. Express* **2013**, *21*, 1317–1323. [[CrossRef](#)]
3. Du, Z.; Zhang, S.; Li, J.; Gao, N.; Tong, K. Mid-infrared tunable laser-based broadband fingerprint absorption spectroscopy for trace gas sensing: A review. *Appl. Sci.* **2019**, *9*, 338. [[CrossRef](#)]
4. Von Edlinger, M.; Scheuermann, J.; Nähle, L.; Zimmermann, C.; Hildebrandt, L.; Fischer, M.; Koeth, J.; Weih, R.; Höfling, S.; Kamp, M. DFB interband cascade lasers for tunable laser absorption spectroscopy from 3 to 6 μm. In Proceedings of the Volume 8993, Quantum Sensing and Nanophotonic Devices XI, SPIE OPTO, San Francisco, CA, USA, 31 January 2014. [[CrossRef](#)]
5. Bewley, W.W.; Canedy, C.L.; Kim, C.S.; Kim, M.; Merritt, C.D.; Abell, J.; Vurgaftman, I.; Meyer, J.R. High-power room-temperature continuous-wave mid-infrared interband cascade lasers. *Opt. Express* **2012**, *20*, 20894–20901. [[CrossRef](#)] [[PubMed](#)]
6. Jung, D.; Bank, S.; Lee, M.L.; Wasserman, D. Next-generation mid-infrared sources. *J. Opt.* **2017**, *19*, 123001. [[CrossRef](#)]
7. Cerutti, L.; Vicet, A.; Tournié, E. Interband mid-infrared lasers. In *Mid-Infrared Optoelectronics*; Tournié, E., Cerutti, L., Eds.; Woodhead Publishing: Duxford, UK, 2020; pp. 91–130. [[CrossRef](#)]
8. Rogalski, A. HgCdTe infrared detector material: History, status and outlook. *Rep. Prog. Phys.* **2005**, *68*, 2267. [[CrossRef](#)]
9. Melngailis, I.; Strauss, A.J. SPONTANEOUS AND COHERENT PHOTOLUMINESCENCE IN Cd_xHg_{1-x}Te. *Appl. Phys. Lett.* **1966**, *8*, 179–180. [[CrossRef](#)]
10. Bleuse, J.; Bonnet-Gamard, J.; Mula, G.; Magnea, N.; Pautrat, J.L. Laser emission in HgCdTe in the 2–3.5 μm range. *J. Cryst. Growth* **1999**, *197*, 529–536. [[CrossRef](#)]
11. Roux, C.; Hadji, E.; Pautrat, J.L. 2.6 μm optically pumped vertical-cavity surface-emitting laser in the CdHgTe system. *Appl. Phys. Lett.* **1999**, *75*, 3763–3765. [[CrossRef](#)]
12. Arias, J.M.; Zandian, M.; Zucca, R.; Singh, J. HgCdTe infrared diode lasers grown by MBE. *Semicond. Sci. Technol.* **1993**, *8*, S255. [[CrossRef](#)]
13. Popov, A.; Sherstnev, V.; Yakovlev, Y.; Mücke, R.; Werle, P. High power InAsSb/InAsSbP double heterostructure laser for continuous wave operation at 3.6 μm. *Appl. Phys. Lett.* **1996**, *68*, 2790–2792. [[CrossRef](#)]
14. Malin, J.I.; Meyer, J.R.; Felix, C.L.; Lindle, J.R.; Goldberg, L.; Hoffman, C.A.; Bartoli, F.J.; Lin, C.H.; Chang, P.C.; Murry, S.J.; et al. Type II mid-infrared quantum well lasers. *Appl. Phys. Lett.* **1996**, *68*, 2976–2978. [[CrossRef](#)]
15. Haug, A. Auger recombination in direct-gap semiconductors: Band-structure effects. *J. Phys. C Solid State Phys.* **1983**, *16*, 4159. [[CrossRef](#)]
16. Abakumov, V.N.; Perel, V.I.; Yassievich, I.N. *Nonradiative Recombination in Semiconductors*; Elsevier: Amsterdam, The Netherlands, 1991; pp. 191–197.
17. Utochkin, V.V.; Kudryavtsev, K.E.; Fadeev, M.A.; Razova, A.A.; Bykov, D.S.; Aleshkin, V.Y.; Dubinov, A.A.; Mikhailov, N.N.; Dvoretzky, S.A.; Rumyantsev, V.V.; et al. Mid-IR stimulated emission in Hg(Cd)Te/CdHgTe quantum well structures up to 200 K due to suppressed Auger recombination. *Laser Phys.* **2020**, *31*, 015801. [[CrossRef](#)]

18. Kudryavtsev, K.E.; Rummyantsev, V.V.; Aleshkin, V.Y.; Dubinov, A.A.; Utochkin, V.V.; Fadeev, M.A.; Mikhailov, N.N.; Alymov, G.; Svintsov, D.; Gavrilenko, V.I.; et al. Temperature limitations for stimulated emission in 3–4 μm range due to threshold and non-threshold Auger recombination in HgTe/CdHgTe quantum wells. *Appl. Phys. Lett.* **2020**, *117*, 083103. [[CrossRef](#)]
19. Fadeev, M.A.; Rummyantsev, V.V.; Kadykov, A.M.; Dubinov, A.A.; Antonov, A.V.; Kudryavtsev, K.E.; Dvoretzkii, S.A.; Mikhailov, N.N.; Gavrilenko, V.I.; Morozov, S.V. Stimulated emission in the 2.8–3.5 μm wavelength range from Peltier cooled HgTe/CdHgTe quantum well heterostructures. *Opt. Express* **2018**, *26*, 12755–12760. [[CrossRef](#)]
20. Fadeev, M.A.; Troshkin, A.O.; Dubinov, A.A.; Utochkin, V.V.; Razova, A.A.; Rummyantsev, V.V.; Aleshkin, V.Y.; Gavrilenko, V.I.; Mikhailov, N.N.; Dvoretzky, S.A.; et al. Mid-infrared stimulated emission in HgCdTe/CdHgTe quantum well heterostructures at room temperature. *Opt. Eng.* **2020**, *60*, 082006. [[CrossRef](#)]
21. Utochkin, V.V.; Fadeev, M.A.; Kudryavtsev, K.E.; Rummyantsev, V.V.; Razova, A.A.; Morozova, E.E.; Shengurov, D.V.; Mikhailov, N.N.; Dvoretzky, S.A.; Morozov, S.V. Mid-IR lasing up to 260 K in HgCdTe/CdHgTe QW structure with microdisk resonators under optical pumping. In Proceedings of the Abstract Digest of Infrared, Millimeter and Terahertz Waves 2021, Chengdu, China, 29 August–3 September 2021. [[CrossRef](#)]
22. Dvoretzky, S.; Mikhailov, N.; Sidorov, Y.; Shvets, V.; Danilov, S.; Wittman, B.; Ganichev, S. Growth of HgTe quantum wells for IR to THz detectors. *J. Electron. Mater.* **2010**, *39*, 918–923. [[CrossRef](#)]
23. Kudryavtsev, K.E.; Rummyantsev, V.V.; Utochkin, V.V.; Fadeev, M.A.; Aleshkin, V.Y.; Dubinov, A.A.; Zholudev, M.S.; Mikhailov, N.N.; Dvoretzkii, S.A.; Remesnik, V.G.; et al. Toward Peltier-cooled mid-infrared HgCdTe lasers: Analyzing the temperature quenching of stimulated emission at $\sim 6 \mu\text{m}$ wavelength from HgCdTe quantum wells. *J. Appl. Phys.* **2021**, *130*, 214302. [[CrossRef](#)]
24. Shaklee, K.L.; Nahory, R.E.; Leheny, R.F. Optical gain in semiconductors. *J. Lumin.* **1973**, *7*, 284–309. [[CrossRef](#)]
25. Rummyantsev, V.V.; Fadeev, M.A.; Aleshkin, V.Y.; Dubinov, A.A.; Utochkin, V.V.; Antonov, A.V.; Ryzhov, D.A.; Kuritsin, D.I.; Gavrilenko, V.I.; Krasilnik, Z.F.; et al. Terahertz emission from HgCdTe QWs under long-wavelength optical pumping. *J. Infrared Millim. Terahertz Waves* **2020**, *41*, 750–757. [[CrossRef](#)]
26. Meyer, J.R.; Canedy, C.L.; Kim, M.; Kim, C.S.; Merritt, C.D.; Bewley, W.W.; Vurgaftman, I. Comparison of Auger coefficients in type I and type II quantum well midwave infrared lasers. *IEEE J. Quantum Electron.* **2021**, *57*, 1–10. [[CrossRef](#)]